

Slow-Neutron Capture Gamma Rays from Sodium and Cadmium*

HENRY T. MOTZ†

Brookhaven National Laboratory, Upton, New York

(Received August 15, 1956)

A thin-lens magnetic spectrometer has been used to observe the external conversion spectra of $\text{Na}^{23}(n,\gamma)\text{Na}^{24}$ and $\text{Cd}^{113}(n,\gamma)\text{Cd}^{114}$ and the internal conversion spectrum of $\text{Cd}^{113}(n,\gamma)\text{Cd}^{114}$ in the energy range of 300 keV to 3 MeV. An arrangement using an external neutron beam and one using a source located inside the reactor are compared. It is shown that target materials placed inside the reactor allow a better discrimination against background and permit the use of a K x-ray-conversion-electron coincidence scheme for photoelectric conversion which greatly simplifies the observed conversion spectrum. Four of the nine gamma rays observed from sodium are assigned to transitions on the basis of the known energy levels from $\text{Na}^{23}(d,\beta)\text{Na}^{23}$; the other five are assigned to probable transitions on an energy and intensity basis. The internal conversion spectrum of Cd^{114} has disclosed a $0+$ level at 1308 ± 3 keV and the de-excitation of this level by means of $E2$ transitions to other states in Cd^{114} is also observed. Three other states in Cd^{114} are proposed in addition to the well-known 559-keV ($2+$) and 1286-keV ($4+$) states to explain the observed gamma-ray spectrum: 1212 ± 3 keV ($2+$ or $1+$), 1368 ± 4 keV ($2+$ or $1+$), and 1860 ± 5 keV ($4+$ or $3+$).

1. INTRODUCTION

THERMAL neutron absorption is usually accompanied by gamma-ray emission from the compound nucleus, the emission of charged particles being confined to a few light elements and the fissionable elements. Some of the earliest work on neutron absorption indicated the presence of neutron-capture gamma radiation, which has been called the "prompt" radiation to distinguish it from the radiation from any radioactivity of the residual nucleus. The capture gamma-ray spectrum of an isotope can yield information concerning the disintegration scheme of the residual nucleus although it is usually necessary to have some other information concerning the residual nucleus to assign an observed line to a particular transition. In order to fit the observed lines into a reliable decay scheme an accurate measure of energies and an approximate measure of intensities for each of the lines is required, and these requirements become more and more severe as the complexity of the spectrum increases. Since the average multiplicity of most (n,γ) reactions is about 4,¹ it is possible to excite low-lying levels over a spin range of several units even for dipole emission in the first two or three cascade transitions. Thus it is to be expected that low-lying levels, which might not appear in a radioactive decay scheme because of energy or spin limitations, will be excited following neutron absorption. For intermediate and heavy nuclei, the high-level density above 2 or 3 MeV will tend to cause the appearance of a great number of weak low-energy transitions in the spectrum, but a high-intensity low-energy line (<1 – 2 MeV) will most probably correspond to transitions between low-lying levels.

The prompt gamma radiation following neutron capture has been studied by almost every known

method of measuring gamma-ray energies, and a summary of the early work appears in a review article by Kinsey.² All of the experiments prior to 1950 were of low resolution and reveal few details of the spectra. In 1950 Bell and Elliot³ used a thin-lens magnetic spectrometer for the measurement of the $\text{H}^1(n,\gamma)\text{H}^2$ gamma-ray energy by means of photoelectric conversion with a line width of 3%. The background in their experiment relative to the K photoelectric peak was high, but this approach seemed to show promise if the background could be reduced. Kinsey and Bartholomew² have used a pair spectrometer, obtaining data above 3 MeV for elements having cross sections as low as 5 millibarns. Groshev, Adyasevich, and Demidov^{4,5} have used a Compton spectrometer with high sensitivity from about 300 keV to 10 MeV with a resolution of 2.3%.

This paper presents data taken with a thin-lens spectrometer on the Compton and photoelectric external conversion spectra of $\text{Na}^{23}(n,\gamma)\text{Na}^{24}$ and $\text{Cd}^{113}(n,\gamma)\text{Cd}^{114}$ and on the internal conversion spectrum of $\text{Cd}^{113}(n,\gamma)\text{Cd}^{114}$. Preliminary results on this work have been previously reported.⁶⁻⁸ Two basic arrangements were used for the source and spectrometer geometry. In the first, Arrangement *A*, a target was placed inside the spectrometer at the point where an external neutron

² B. B. Kinsey in *Beta- and Gamma-Ray Spectroscopy*, edited by K. Siegbahn (North Holland Publishing Company, Amsterdam, 1955), Chap. 25.

³ R. E. Bell and L. G. Elliot, *Phys. Rev.* **79**, 282 (1950).

⁴ Groshev, Adyasevich, and Demidov, *Proceedings of the International Conference on the Peaceful Uses of Atomic Energy, Geneva, 1955* (Columbia University Press, New York, 1956), Vol. 2, p. 39.

⁵ Adyasevich, Groshev, and Demidov, *Conference of the Academy of Sciences of the USSR on the Peaceful Uses of Atomic Energy, July 1-5, 1955, Session of the Division of Physico-Mathematical Sciences* (Academy of Science, Moscow, 1955. English translation: Consultants Bureau, New York, 1956), p. 195.

⁶ Thornton, der Mateosian, Motz, and Goldhaber, *Phys. Rev.* **86**, 604 (1952).

⁷ H. T. Motz, *Phys. Rev.* **90**, 355 (1953); **99**, 656 (1955).

⁸ A. W. McReynolds, *Proceedings of the International Conference on the Peaceful Uses of Atomic Energy, 1955* (Columbia University Press, New York, 1956), Vol. 2, p. 94.

* Work performed under the auspices of the U. S. Atomic Energy Commission.

† Now at Los Alamos Scientific Laboratory, Los Alamos, New Mexico.

¹ C. O. Muehlhause, *Phys. Rev.* **79**, 277 (1950).

beam crossed the axis of the spectrometer. This arrangement is similar to that usually employed with a radioactive source in that the source is small and is placed as close as possible to the converter foil. In the second, Arrangement *B*, the target material was placed inside the reactor, and a gamma-ray beam was brought out through the reactor shield and along the axis of the spectrometer. This second arrangement is different in that the gamma rays passing through the converter are highly collimated. Collimation alters the sensitivity of any type of spectrometer and allows the design of types of spectrometers different from those that are possible for uncollimated radiation. A high-intensity source is needed to attain this collimation, but for the geometry of this experiment Arrangement *B* allows an increase in yield for small neutron absorption cross-section materials. The coincidence detection scheme afforded by the collimation also allows a decrease in the relative background and a simplification of the observed conversion spectrum.

2. APPARATUS

The spectrometer was patterned after an instrument described by Hornyak *et al.*⁹ The magnet consists of four 100-turn water-cooled coils having a total resistance of 0.17 ohm. The magnet is driven by a 15-kw generator which furnishes up to 300 amp, a current sufficient to focus 10-Mev electrons. The magnetic field is regulated to within three parts in 10 000 by a galvanometer which measures the potential difference between a

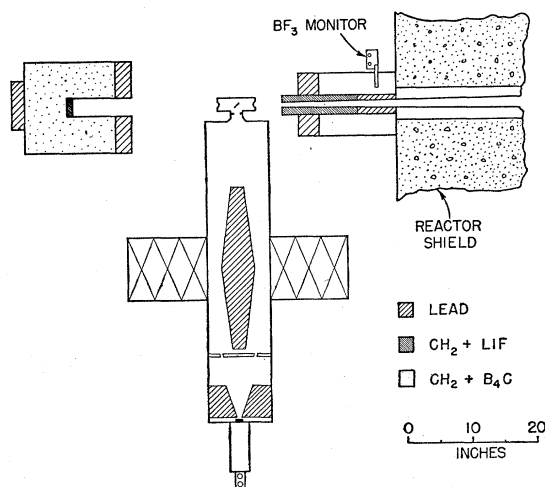


FIG. 1. Arrangement *A*. The neutron beam from the graphite collimator passes through the shielding and target chamber and into the beam catcher. The target material in the neutron beam is placed at the source position of the thin lens spectrometer. The spectrometer electron detector is an anthracene crystal on a 5819 photomultiplier enclosed in a soft-iron magnetic shield. Additional lead shielding and a baffle at the source end of the spectrometer are not shown.

⁹ Hornyak, Lauritsen, and Rasmussen, *Phys. Rev.* **76**, 731 (1949).

series manganin shunt and a potentiometer and whose light beam falls on dual photocells. The generator has a time constant in excess of 0.1 second and a high degree of feedback to the galvanometer was required to attain the desired regulation. Further improvement was obtained by the use of a series inductance and shunt capacity between the generator and the magnet in order to decrease the rapid fluctuations in current due to brush noise.

The electron detector was a thin organic scintillator about 2 cm in diameter and 6 mm thick attached to a 5819 photomultiplier. This type of detector has a low background counting rate but has a nonlinear sensitivity for moderate biases due to the scattering-out of electrons from the scintillator. Although this could be a serious correction for beta spectra, it amounts to only a few percent at 0.5 Mev and is not serious for conversion work. The background can be further reduced by requiring a pulse height corresponding to the energy of the electrons being focused by the spectrometer. This reduces room background and rejects a large fraction of the scattered electrons from the spectrometer walls and baffles. Data are normally taken with and without pulse height analysis on this detector to correct for any drifts in sensitivity.

Data taken with Arrangement *B* used a coincidence analyzer consisting of a dual fast- (~ 0.2 microsecond) and triple slow-coincidence circuits and two single-channel analyzers. The spectrometer is operated automatically and accumulates data for either a fixed time or for a fixed number of neutrons for each magnetic field setting. Long runs required monitoring of room background and magnetic field ripple, and frequent checks were made to assure that no appreciable drifts occurred in the detecting equipment.

3. ARRANGEMENT A

3.1 Experimental Arrangement

A neutron beam of $\sim 10^6$ neutrons/cm² sec from the reactor was collimated by graphite and passed through the target position and into the beam catcher as illustrated in Fig. 1. This geometry allows targets to be easily changed for energy and intensity calibration and a vacuum lock was used for this purpose. External conversion spectra with lead converters were observed for cadmium and boron targets. The arrangement is also useful for the study of internal conversion spectra and could be used for $e\text{-}\gamma$ and $\gamma\text{-}\gamma$ coincidences. The disadvantages of the arrangement for external conversion are: (a) the background is very high relative to K -photoelectric conversion peaks even for high cross-section materials; (b) the target dimensions are limited to approximately the converter diameter which is normally 6 to 12 mm. For moderately low capture cross sections, the fraction of the incident neutrons absorbed becomes small and a rapid decrease in yield occurs for $\sigma < 100$ barns.

3.2 External Conversion Results

The $B^{10}(n,\alpha)Li^7$ reaction is known to emit the 478-keV gamma ray from the first excited state of Li^7 with an intensity of 0.95 gamma per thermal neutron captured.¹⁰ Since the cross section for this reaction is high for thermal neutrons, it is a convenient material to use for low-transmission targets and thus furnishes an excellent calibration line for both energy and intensity. Figure 2 shows the conversion spectrum obtained with a 30-mg/cm² lead converter. The K -photoelectron peak at $H\rho \sim 2400$ gauss-cm is reasonably well resolved from the $L+M$ photopeak and from the Compton electrons. The scintillation detector of the spectrometer was biased to record electrons having an energy greater than 300 keV.

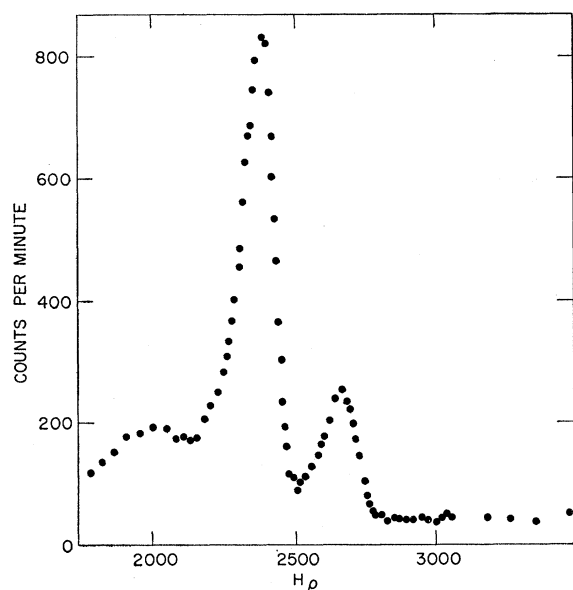


FIG. 2. External conversion spectrum of the 478-keV $B^{10}(n,\alpha)Li^{7*}$ gamma ray observed with Arrangement A. The converter was 30 mg/cm² lead and the K -photoelectron peak is at ~ 2400 gauss-cm.

Figure 3 shows the conversion spectrum of $Cd^{113}(n,\gamma)Cd^{114}$ obtained with the same lead converter for a cadmium target which also had a low transmission. A K photopeak at $H\rho \sim 2700$ gauss-cm, corresponding to a gamma ray of 556 keV, is clearly seen along with its $L+M$ photopeak which is somewhat broader than would be expected from the boron data. Although suggestions of structure above the 556-keV line were consistently indicated, the large background prevented any detailed measurements of additional photoelectric peaks. The comparison of the boron and cadmium data illustrates the large increase in background encountered when the source is emitting high-energy radiations.

¹⁰ Hornyak, Lauritsen, Morrison, and Fowler, *Revs. Modern Phys.* **22**, 291 (1950).

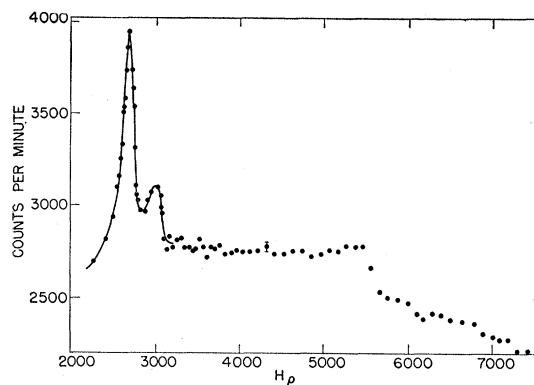


FIG. 3. External conversion spectrum of $Cd^{113}(n,\gamma)Cd^{114}$ under the same conditions as for the data shown in Fig. 2. The discontinuity at ~ 5550 gauss-cm is due to the internal conversion electrons of 1308-keV transition passing through the lead converter. Note the high background relative to that of Fig. 2.

Two comparison measurements were made on the 556-keV line. First its energy and intensity were compared to those of the boron target. Correcting for the change in sensitivity of the photoelectric conversion process with energy yielded an intensity of $0.8_s \pm 0.1$ gamma per neutron captured and the energy measurement was 556 ± 5 keV. A second comparison was made with a source of 50-day In^{114m} which is known to emit two cascade gamma rays of 556 ± 1 and 722 ± 1 keV from Cd^{114} .¹¹ Consecutive runs with the same converter showed that the capture gamma ray from cadmium was equal to the 556 line of the radioactive source to within 1 keV.

The external neutron beam was used in conjunction with a NaI scintillation spectrometer to observe the low-energy spectrum from cadmium. Using the 556-keV line as an intensity calibration, (2.7 ± 1) K x-rays and (0.4 ± 0.1) 96-keV gamma rays per 100 disintegrations were observed. Internal conversion from the known gamma rays can account for 1.3 K x-rays per 100 disintegrations leaving an excess of (1.4 ± 1) K x-rays per 100 disintegrations. It is likely that the internal conversion of unobserved weak transitions in the low-energy region are the source of these unassigned x-rays.

3.3 Internal Conversion Results

For elements having large neutron cross sections it is possible to absorb a sufficient fraction of a neutron beam in a thin layer of material to allow the study of the internal conversion electron spectrum. Internal conversion data for several (n,γ) reactions have been reported by Hibdon and Muehlhause¹² and by Church and Goldhaber.¹³ Their results were obtained with

¹¹ Johns, Waterman, MacAskill, and Cox, *Can. J. Phys.* **31**, 325 (1953).

¹² C. T. Hibdon and C. O. Muehlhause, *Phys. Rev.* **88**, 943 (1952).

¹³ E. L. Church and M. Goldhaber, *Phys. Rev.* **95**, 626(A) (1954); E. L. Church (private communication).

high-resolution 180° permanent magnet spectrographs. Cadmium indicated two internally converted gamma rays, one at ~ 96 keV and a weak line at ~ 562 keV.

The internal-conversion electrons from a 10-mg/cm^2 cadmium foil observed with the thin lens is shown in Fig. 4. Relatively strong conversion peaks are seen at 557, 650, and 1305 keV and weak lines at approximately 730 and 800 keV are also indicated. The 556-keV line from Cd^{114} is known to be $E2$ from angular correlation experiments with In^{114} sources¹⁴ and, if it is assumed that this corresponds to the internal conversion peak of the same energy, then the 556-keV line serves as a calibration for the measurement of the number of conversion electrons per disintegration of Cd^{114} . Similarly, if energy equivalence is taken to indicate that the same transition is involved as listed in Table I, then a knowledge of the gamma-ray intensity as obtained from Arrangement B allows the calculation of the total internal conversion coefficient for each line. The results of such a comparison, as listed in Table I, show that the 728- and 808-keV transitions are either $M1$ or $E2$ or $(M1+E2)$, and the 654-keV transition is probably $E2$ but $M1$ cannot be excluded. The 1305-keV electron conversion line is much too intense, however, to correspond to any reasonable multipole. It must therefore come from the internal conversion of a $0^+ \rightarrow 0^+$ transition which is in competition with other decay modes. The externally emitted line of 1298 keV cannot, in this case, correspond to the same transition since unconverted gamma radiation is forbidden for a $0 \rightarrow 0$ transition.

4. ARRANGEMENT B

4.1 Experimental Arrangement

The collimator used to define a narrow gamma-ray beam from a sample placed inside the reactor and the general geometry for the spectrometer as used in Arrangement B is shown in Fig. 5. The sample was located in a section of the reactor well removed from the uranium loading pattern so that the intensity of fast neutrons and fission gamma rays was low in its vicinity. Two 9-mil cadmium foils were sufficient to

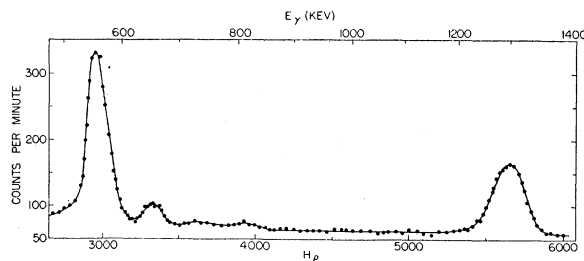


Fig. 4. Internal conversion spectrum of $\text{Cd}^{113}(n,\gamma)\text{Cd}^{114}$ from a 10-mg/cm^2 cadmium foil. The energy scale is based on the K -conversion peaks. L and M conversion lines are not resolved from the K lines.

¹⁴ J. N. Brazos and R. M. Steffen, Phys. Rev. **102**, 753 (1956).

TABLE I. $\text{Cd}^{113}(n,\gamma)\text{Cd}^{114}$ internal conversion.

Internal conversion		External conversion ^a		Internal conversion coefficients ^c $\times 10^3$				
E (keV)	N_e	E (keV)	I	Observed ^b	α_1 $E1$	α_2 $E2$	β_1 $M1$	β_2 $M2$
557 ± 6	1.00	559 ± 2	0.85	...		4.3		
650 ± 6	0.15	654 ± 2	0.23	2.5 ± 0.5	1.0	2.9	3.4	9.5
730 ± 10	~ 0.046	728 ± 3	0.07	2.5 ± 1	0.85	2.2	2.6	7.2
800 ± 10	~ 0.05	808 ± 3	0.09	2.1 ± 1	0.65	1.6	2.0	5.0
1305 ± 8	0.33	1298 ± 5	0.055	$(24 \pm 2)^d$		α_6 3.6	β_4 5.2	β_6 9.0

^a See Table III for complete tabulation of observed lines.

^b Calibration from known $E2$ character of 559-keV line. See reference 14.

^c Theoretical K -conversion coefficients from M. E. Rose, in *Beta- and Gamma-Ray Spectroscopy*, edited by K. Siegbahn (North Holland Publishing Company, Amsterdam, 1955), Chap. 14.

^d See text.

attenuate the slow neutrons emerging from the collimator and the fast neutrons emerging from the 6 to 12 mm outside port were sufficiently low so as to cause no hazard.

This geometry has several advantages over the external source arrangement. (a) The yield of external conversion electrons can be significantly increased by optimizing the geometry for the differential cross section of the conversion process. Detection in the forward direction is the most efficient since the Compton, photoelectric, and pair cross sections are all highly peaked in the forward direction in the MeV region.¹⁵ (b) The high degree of collimation makes it possible to place a gamma-ray detector near the converter but outside of the main beam so that the secondary radiations from the converter can be counted above background. For the Compton effect, the back- and side-scattered gamma rays can be detected and for a high- Z converter such as thorium, the K and L x-rays of the converter material are clearly seen. Each of these radiations is in coincidence with the corresponding conversion electron and can serve as a coincidence trigger for that conversion process. A coincidence system of this type allows the suppression of relative background by a factor of 100 or more and can be used to advantage in simplifying the conversion spectrum. (c) The source intensity available is limited by the self-absorption of gamma radiation in the target material and this limitation is less severe for low cross-section materials than for Arrangement A. For small cross sections and light elements, the internal source allows an increase in yield over the external source arrangement of about 10^3 .

A disadvantage of this internal source arrangement is that the sources are relatively difficult to change since this can be done only when the reactor is shut down and sometimes requires several days of waiting for the decay of highly radioactive sources. Also, the sensitivity is not simple to calculate, for the differential cross section of the conversion process and the electron scattering in the converter must be taken into account. The very low solid angle of the converter seen from the

¹⁵ C. M. Davison and R. D. Evans, Revs. Modern Phys. **24**, 79 (1952).

source ($\sim 10^{-6}$) makes coincidence measurements impossible.

4.2 Compton Effect

The energy of a Compton conversion electron depends on the angle between the conversion electron and the gamma ray being scattered, φ , and is given by

$$E = h\nu \frac{2\alpha}{1 + 2\alpha + (1 + \alpha)^2 \tan^2 \varphi},$$

where α is the energy of the gamma ray in mc^2 units. If a spectrometer detects electrons in the small angular interval $\Delta\varphi$ and at a mean angle $\bar{\varphi}$, the resolution for small angles ($\tan\varphi \sim \varphi$) is

$$\frac{\Delta E}{E} \sim \frac{(1 + \alpha)^2 [2(\Delta\varphi) \bar{\varphi} + (\Delta\varphi)^2]}{1 + 2\alpha + (1 + \alpha)^2 \bar{\varphi}^2}.$$

For the case in which $\Delta\varphi \ll \bar{\varphi}$ it is seen that the energy spread for a given $\Delta\varphi$ due to the angular effects alone increases approximately linearly with $\bar{\varphi}$. For the more usual case where the electrons emitted between 0° and an upper limit $\Delta\varphi$ are detected, the resolution varies as the second term, $(\Delta\varphi)^2$. The energy spread for $\alpha = 2$, $\bar{\varphi} = 12^\circ$, and $\Delta\varphi = 4^\circ$ is $\sim 4\%$ which is about the condition expected for the lens spectrometer with an infinitely thin converter. The observed resolution in an actual case would be given by the angular energy spread combined with the energy losses in the converter and the resolution of the spectrometer. The range of angles $\Delta\varphi$ is determined by the gamma-ray beam collimation, the apertures of the spectrometer, and the electron scattering in the converter. The latter effect can become quite serious at low energies and not only increases the half-width of the observed energy distribution

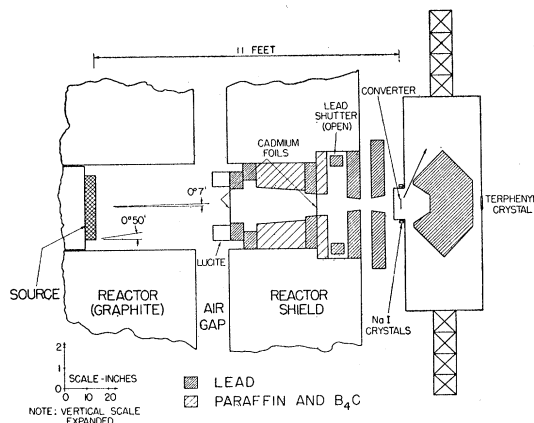


FIG. 5. Arrangement B. The target material is placed inside the reactor. The gamma-ray collimator inside and just outside the reactor shield collimates the gamma-ray beam to 6- to 12-mm diameter depending upon the converter size. The photomultipliers used for the spectrometer electron detector and for the x-ray detectors along with their magnetic covers and lead shielding are not shown.

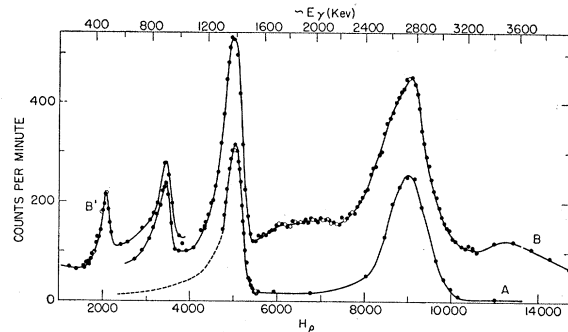


FIG. 6. Compton conversion spectrum from $\text{Na}^{23}(n,\gamma)\text{Na}^{24}$ and $\text{Na}^{24}(\beta,\gamma)\text{Mg}^{24}$ observed in Arrangement B with a 25-mg/cm² beryllium converter. Curve A: reactor off—showing Mg^{24} gamma rays in approximate equilibrium. Curve B: reactor on—with terphenyl electron detector biased at ~ 500 keV. Curve B': reactor on—with terphenyl electron detector biased at ~ 200 keV.

but greatly increases the relative yield in the low-energy tail owing to the scattering-in of low-energy electrons. This effect is illustrated in the data of Motz *et al.*¹⁶ in the case of Na^{24} observed with an 11-mil Be converter (see Fig. 6, reference 16). The requirement of a backscattered gamma ray in coincidence with the forward-scattered electron can be used to eliminate this scattered-in effect because the *initial* angle of emission of the electron is related to the angle of the backscattered gamma ray. Suitable angular limits on the detection of the scattered gamma ray thus restricts the coincidence yields to a corresponding range of *initial* electron angles and prevents the coincidence detection of low-energy scattered-in electrons.

The Compton conversion-electron spectrum from a Na_2CO_3 sample placed in the reactor is shown in Fig. 6. The converter was 25 mg/cm² Be and the over-all resolution obtained was about 10%. The two strong peaks are from Mg^{24} following the beta decay of 12.6-hour Na^{24} . Curve A shows these two peaks when the reactor is off. Curves B and B' show the corresponding spectrum when the reactor is on and the Na^{24} is in equilibrium. Two distinct low-energy peaks are seen corresponding to gamma rays of approximately 470 and 870 keV. Weaker unresolved lines are present in the region of both the 1368-keV and 2760-keV Mg^{24} lines as well as between and above these lines. The resolution is too poor to give any reliable measure of these smaller Compton peaks, however. The spectrum of $\text{Cd}^{113}(n,\gamma)\text{Cd}^{114}$ taken with a 50-mg/cm² Be converter, better spectrometer resolution, and smaller $\Delta\varphi$ is shown in Fig. 7 both for singles and coincidence detection. The two NaI(Tl) scintillation detectors used for the backscattered gamma-ray coincidence counters were located 1 inch from the center-line of the gamma-ray beam and were 6 mm thick. The geometry limited the gamma-ray detection from 120° to 160° with respect to the incident gamma-ray beam and the efficiency of

¹⁶ J. W. Motz *et al.*, *Rev. Sci. Instr.* **24**, 929 (1953).

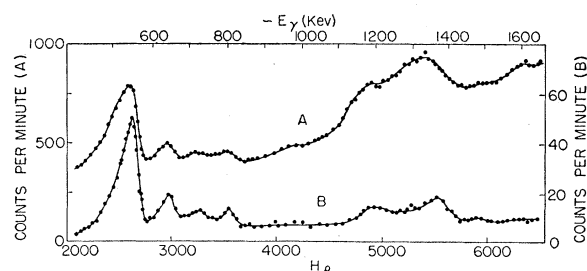


FIG. 7. $\text{Cd}^{113}(n,\gamma)\text{Cd}^{114}$ Compton conversion spectrum observed with Arrangement B using a 50-mg/cm² beryllium converter. Curve A: singles detection as for the data shown in Fig. 6. Curve B: coincidence spectrum—two 6-mm NaI crystals were used to detect the backscattered gamma rays in the 120°–160° cone.

detecting the backscattered gamma rays was about 0.15 in this cone. Since the gamma-ray detectors were inefficient even in this cone, the coincidence counting rate was quite low. The results indicate at least four peaks in the range of 550- to 800-keV gamma-ray energy and perhaps three unresolved peaks in the 1200- to 1400-keV region. The coincidence spectrum is seen to have a somewhat better resolution and a decreased low-energy tail with respect to the singles spectrum owing to the rejection of low-energy scattered-in electrons as discussed in the foregoing. The resolution for the coincidence spectrum was about 5%, which is the best that could be obtained with this geometry.

Although the yield for Compton conversion is comparable to that from photoelectric conversion above 500 keV, the resolution is inferior for the geometry of the thin lens and for this reason Compton data were taken only for sodium and cadmium. Compton conversion is capable of good resolution for a spectrometer which detects conversion electrons emitted in a small cone in the forward direction. The sensitivity of such a spectrometer increases with energy. Compton spectrometers used in this way have operated at 2 to 3% resolution.^{4,16–18} A further improvement of resolution to about 1% without a severe sacrifice in sensitivity could be obtained for reactor-activated sources by the use of a high-resolution spectrometer in conjunction with the coincidence detection of the backscattered gamma ray.

4.3 Photoelectric Effect

The differential cross section for the photoelectric effect has been calculated by Sauter¹⁹ for relativistic energies by using the Born approximation and indicates that the cross section is highly directional in the MeV region. Although the approximation requires that $Z \ll 137$, the experimental observations of Hultberg²⁰ for gold using gamma rays of 411, 660, and 1330 keV indicate that the angular position of the maximum in the

¹⁷ M. Mladjenovic and A. Hedgran, *Arkiv Fysik* **8**, 49 (1954).

¹⁸ Dzelepov, Zhukovskii, Karamian, and Shestopalova, *Izvest. Akad. Nauk S.S.S.R.* **17**, 517 (1953).

¹⁹ F. Sauter, *Ann. Physik* **11**, 454 (1931). See reference 15.

²⁰ S. Hultberg, *Arkiv Fysik* **9**, 245 (1955).

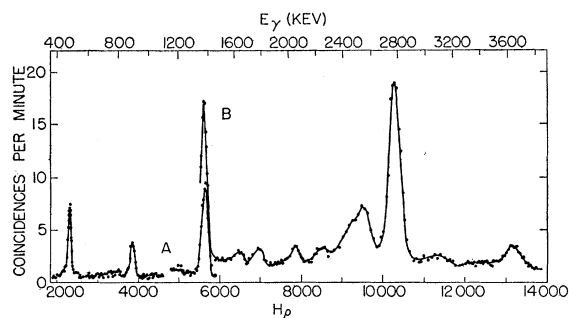


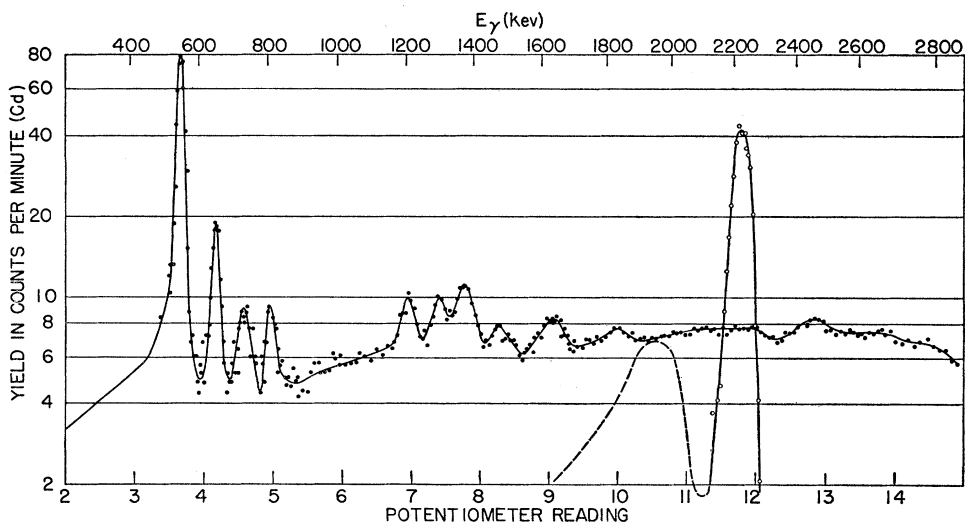
FIG. 8. $\text{Na}^{23}(n,\gamma)\text{Na}^{24}$ and $\text{Na}^{24}(\beta,\gamma)\text{Mg}^{24}$ photoelectron coincidence spectrum observed with Arrangement B. Two 6-mm NaI crystals were used to detect the K x-rays of the converter. Curve A: 22-mg/cm² thorium converter. Curve B: 44-mg/cm² uranium converter.

cross section is in reasonable agreement with the values calculated from Sauter's expression. Since the average scattering angle in the converters in the capture gamma-ray observations is ~ 20 degrees, the details of the differential cross-section dependence need not be known with high accuracy and it was felt that the expression due to Sauter would be acceptable for sensitivity calculations.

The expected photoelectric sensitivity with energy has been calculated for the thin-lens acceptance angle of 12 degrees by using Sauter's expression for the differential cross section and assuming that the scattering distribution was Gaussian. Cross-section curves for gamma rays of 500 to 3000 keV were integrated for Gaussian scattering distributions having $w(e^{-1})$ values of 5 to 50 degrees. These results were then plotted versus w^2 and integrated up to the maximum value expected for the various converters used. An average value of the effective cross section for converters of thorium and uranium for thicknesses of 20 to 50 mg/cm² indicated that the sensitivity varied as $\sim E^{-1}$ from 0.5 to 3.0 MeV. The observed ratio of the 1.38- and 2.76-MeV gamma rays of Mg^{24} when corrected for self-absorption agreed with the calculated ratio to within 15%. Since the statistical accuracy of observed lines is often of this order, the calculated sensitivity curve was used for all intensity determinations.

The K photoelectric conversion process is accompanied by the emission of a K x-ray of the converter material. The x-rays are isotropic in direction, are emitted in 10^{-15} second, and the energy is characteristic of the converter and not of the gamma ray causing the conversion. These K x-rays can be efficiently detected and serve as excellent coincidence triggers for the K photoelectric conversion process. Two NaI(Tl) detectors were used to detect these K x-rays which are found to be about 5 times the background for a 3-mm crystal placed 2 cm off the center-line of a 6-mm diameter gamma-ray beam. A single-channel analyzer is used to select pulse heights from these crystals corresponding to the x-ray energy. In this manner, L+M conversion

FIG. 9. $\text{Cd}^{113}(n,\gamma)\text{Cd}^{114}$ and $\text{H}^1(n,\gamma)\text{H}^2$ photoelectron coincidence spectrum observed with Arrangement B and a 44-mg/cm² uranium converter. The cadmium source was an array of 9-mil foils inside a 3×3×5-in. box. The hydrogen source was a 325-gram sample of polyethylene. Two 3-mm NaI crystals used for x-ray detection.



peaks are completely eliminated and the general background is highly suppressed. For the angles encountered with these geometrical conditions, the side-scattered gamma ray from a Compton conversion is greater than 160 keV for gamma rays of >500 keV. The Compton-scattered gamma-ray peak is sufficiently separated from the x-ray peak to allow a single-channel analyzer to accept only the x-ray peak. A scintillation detector occasionally produces a small pulse from a Compton-scattered gamma ray that falls into the x-ray gate, however, and thus if the Compton electron is detected by the spectrometer a true coincidence is recorded. The Compton electron peak is suppressed by a factor of about 10 by this coincidence method. The two Mg^{24} lines shown in Fig. 8 and the 2230-keV line from $\text{H}^1(n,\gamma)\text{H}^2$ shown in Fig. 9 illustrate this suppression.

4.4 Results

The external conversion-electron- K x-ray coincidence spectrum obtained for $\text{Na}^{23}(n,\gamma)\text{Na}^{24}$ is shown in Fig. 8. The equilibrium intensity of the 1368- and 2760-keV lines of Mg^{24} from the radioactive decay of Na^{24} were used for energy and intensity calibration. Ten conversion peaks were observed in addition to the two Mg^{24} lines and one of these (1781 keV) was due to Si^{28} from the radioactive decay of the Al^{28} produced in the container. The energies and intensities of the nine Na^{24} lines are listed in Table II along with the possible assignment based on the $\text{Na}^{23}(d,p)\text{Na}^{24}$ Q values.²¹ The capture gamma-ray measurements of Groshev *et al.*⁴ and of Braid²² are also listed for comparison. Because of the low counting rate encountered in this work, it was not possible to scan the 1376- and 2760-keV regions before the Mg^{24} lines grew in, and thus no prompt Na^{24} lines could be detected in these regions.

²¹ A. Sperduto and W. W. Buechner, *Phys. Rev.* **88**, 574 (1952).

²² T. H. Braid, *Phys. Rev.* **102**, 1109 (1956).

Some of the cadmium coincidence data obtained are shown in Figs. 9, 10, and 11. The $\text{H}^1(n,\gamma)\text{H}^2$ line of 2230 keV³ was observed from a sample of polyethylene with the same conditions as the cadmium run illustrated in Fig. 9 and is also shown in that figure. The hydrogen capture line best illustrates the simple coincidence spectrum and low background obtained from the experimental arrangement. A larger cadmium source and better spectrometer resolution were used in obtaining the data illustrated in Figs. 10 and 11 and several lines are more clearly resolved because of these improvements. The external conversion results for cadmium are listed in Table III.

5. CONCLUSIONS

5.1 Sodium

The energy levels of Na^{24} are known to an excitation of 4600 keV from the accurate measurements of Sperduto and Buechner²¹ on the $\text{Na}^{23}(d,p)\text{Na}^{24}$ reaction. The ground state Q value combined with the binding energy of the deuteron indicates that the capture of a slow neutron leads to the formation of an excited state in Na^{24} at 6958 ± 8 keV. Kinsey *et al.*²³ and Groshev *et al.*⁴ are in agreement in that no excitation of the ground state direct from the capturing state, transition (C)–(0), is observed in the (n,γ) reaction, nor is the transition (C)–(1) observed, but the transitions (C)–(2), (C)–(3), and (C)–(4) are observed and have intensities of 21%, 6%, and 1–2% per neutron captured, respectively. The level numbers for the excited states correspond to those assigned by Sperduto and Buechner. Groshev reports a high-energy line corresponding energetically to the transition (C)–(6) with an intensity of $\sim 2.1\%$. It is not certain that the weak lines observed by Groshev *et al.* are necessarily

²³ Kinsey, Bartholomew, and Walker, *Phys. Rev.* **83**, 519 (1951).

TABLE II. $\text{Na}^{23}(n,\gamma)\text{Na}^{24}$ external conversion.

Present work		Transition ^b	ΔE_c (<i>d,p</i>)	Groshev ^d		Braid ^e	
<i>E</i> (keV)	<i>I</i> ^a			<i>E</i> (keV)	<i>I</i>	<i>E</i> (keV)	<i>I</i>
473±4	50±10	(1)–(0)	472±8	470±15	74	480±20	60
		(17)–(12)	464±11	(710±15)	5		
877±5	30±10	(3)–(1)	869±9	860±10	44	860±20	34
		(8)–(7)	848±11	1350±10	6.5	1350±30	6
1630±8	10	(16)–(7)	1623±11	1660±10	7.5	1660±50	5
		(17)–(7)	1641±11	(1870±30)	5.5		
1900±20	~3	(5)–(0)	1884±11	(1950±30)	4		
		(6)–(2)	1900±11				
2030±10	13	(12)–(4)	1894±11	2020±15	11.5	2020±30	12
		(7)–(2)	1997±11				
2210±15	8	(6)–(1)	1992±11	2210±30	7.5		
		(13)–(4)	2006±11	2410±30	10.5		
2510±15	~15	(14)–(5)	2015±11	2520±20	21	2530±30	19
		(15)–(5)	2045±11				
3070±20	7	(14)–(4)	2055±11	2840±20	7.		
		(10)–(2)	3059±11	3080±20	9.5		
3590±25	18	(C)–(14)	3059±11	3300±20	5.		
		(C)–(13)	3108±11				
3590±25	18	(9)–(0)	3582±8	3560±30	18	3560±50 ^f	20
		(16)–(2)	3620±8	3600±30		3600±30 ^f	10
		(C)–(8)	3549±8				

^a Intensity in gamma rays per 100 neutrons absorbed.

^b Level numbers from reference 21. (C) refers to capture state at 6958 keV.

^c Energy of indicated transition from (*d,p*) level measurements of reference 21.

^d Groshev, Advasevich, and Demidov, reference 4. Parentheses denote a doubtful line.

^e T. H. Braid, reference 22.

^f Kinsey, Bartholomew, and Walker, reference 23.

due to $\text{Na}^{23}(n,\gamma)\text{Na}^{24}$ since NaF was used for target material and the slow-neutron absorption of F is ~1.8% of that of Na. Both Kinsey *et al.* and Groshev *et al.* report lines at 3560 and 3600 keV which are not clearly resolved and they assign a total intensity to these two lines of 20–30%.

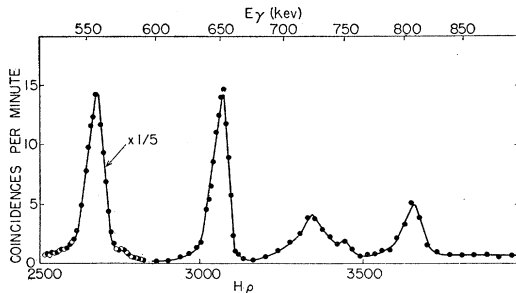


FIG. 10. $\text{Cd}^{113}(n,\gamma)\text{Cd}^{114}$ photoelectric coincidence conversion spectrum observed in Arrangement B with a 22-mg/cm² thorium converter and a 3×3×48-in. array of 3-mil cadmium foils.

Four of the low-energy transitions observed in the present work can be assigned to definite transitions by energy comparison with the (*d,p*) *Q*-value differences as is indicated in Table II. The energies and assigned transitions for these four lines are 473: (1)–(0); 877: (3)–(1); 2210: (9)–(3); and 2510: (13)–(3). In addition to these four lines it can be shown that the 1630-keV line agrees in energy only with the transitions (16)–(7) or (17)–(7).

On the basis of the above assignments one can attempt to account for the excitation and de-excitation of the levels involved by assigning the remaining lines observed. This requires a consideration of both energy agreement with the (*d,p*) *Q*-value differences and the intensity balance for each level that must result if the decay scheme is complete. The following points then arise:

(i) Level (1) is populated only by the 30–40% transition (3)–(1) in the energy range above 300 keV.

The de-excitation of (1) to the ground state is greater than 50%, so the predicted 92-keV transition (2)–(1) must occur with an appreciable intensity to explain the added population of (1) and also the decay of (2). The population of (2) is 21% due to the transition (C)–(2), so the 92-keV transition must account for at least 21% excitation of this state. A gamma ray of approximately 90 keV has been observed with a NaI scintillation spectrometer using an external thermal neutron beam in agreement with this predicted transition.

(ii) Level (3) decays by means of transition (3)–(1) with an intensity of 30%. Level (3) is populated by means of (C)–(3), (9)–(3), and (13)–(3), which total to 30% in agreement with the decay intensity.

(iii) Level (4) is populated to 1–2%, but the low-energy lines observed in the present work do not account for the de-excitation of this state. The low intensity expected can account for missing the expected decay lines. Groshev *et al.*⁴ report a line of $\sim 5\%$ intensity of 1870 keV which could be from transition (4)–(0).

(iv) Level (6) is populated to 2% by means of (C)–(6) and the only transition observed that will account for the decay of this level is the 1900-keV line of 3% which fits with the transition (6)–(2).

(v) Level (7) is populated by the 10% transition (16,17)–(7) and the de-excitation of this state can be accounted for by assigning the 13% line of 2030 keV to transition (7)–(2).

(vi) Level (9) decays by means of the 8% transition (9)–(3) and the 5% line of 3300 keV observed by Groshev *et al.* can account for some of the excitation of (9) if assigned to transition (C)–(9). The 3590-keV line observed in the present work consists of two unresolved lines according to both Kinsey *et al.* and Groshev *et al.*, as is indicated in Table II. Both Braid and Groshev assign the 3560-keV line to transition (C)–(8) and the energy difference of this transition does indeed agree with the observed energy. One must then account for the decay of level (8) with one or more transitions totaling 10–20% and present data do not disclose any such decays. The assignment (9)–(0) for this line is indicated in Fig. 12 and is preferred even though the excitation of (9) cannot be accounted for. The excitation of (9) involves transitions between levels of greater than 3600 keV and it seems much more likely that these excitation transitions would be missed than those corresponding to the decay of the state (8) at 3409 keV.

These points emphasize the lack of completeness of the decay scheme illustrated in Fig. 12 and indicate the need for measurements of higher precision in both energy and intensity. Coincidence experiments would be helpful in clearing up many of the doubtful assignments made here but moderately good resolution would be required to determine many assignments uniquely.

The beta decay of Ne^{24} has been shown by Dropesky

TABLE III. $\text{Cd}^{113}(n,\gamma)\text{Cd}^{114}$ external conversion.

Present work		Adyasevich ^b		Johns ^c
E_γ (keV)	I_γ^a	E_γ (keV)	I_γ	E_γ (keV)
559 ± 2	85	560 ± 10	42	556 ± 1
576 ± 4	~ 7			
654 ± 2	23	660 ± 10	14	
728 ± 3	6.5	730 ± 10	7.5	722 ± 1
752 ± 5	2.5	(760 ± 20)	2	
808 ± 3	9.3	820 ± 10	7	
1210 ± 5	6.5	1230 ± 15	4	
1298 ± 5	5.7	1310 ± 20	4	
1370 ± 5	11.6	1370 ± 20	5	
1403 ± 5	5.5	1420 ± 20	3	
1498 ± 5	4.4	1520 ± 20	3	
1660 ± 10	6	1630 ± 20	3	
		1790 ± 20	2	
(1845 ± 15)	~ 3	1820 ± 20	...	
		1870 ± 20	...	
(~ 1960)	~ 2.5			
		2115 ± 30	...	
		2280 ± 30	...	
(2455 ± 15)	~ 3	2450 ± 20	5	

^a Intensity in gamma rays per 100 neutrons absorbed.

^b Adyasevich, Groshev, and Demidov, reference 5.

^c Johns, Waterman, MacAskill, and Cox, reference 11.

and Schardt²⁴ to consist of allowed beta transitions to states (1) and (3) but not to the ground state (0) or the excited state (2). This information along with the $M3$ nature of the 472-keV transition (1)–(0)²⁴ and the known $4+$ ground state allows the spin and parity assignments for states (1), (2), and (3) of $1+$, $\geq 2+$, and $1+$ to be made. A $2+$ assignment for state (2) is made since this state is excited by the transition (C)–(2) from the $2+$ (or $1+$) state (C) and the transition (2)–(0) to the $4+$ ground state has not been observed. These assignments of $1+$, $2+$, and $1+$

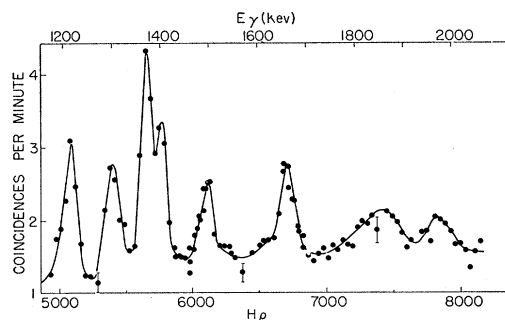


FIG. 11. $\text{Cd}^{113}(n,\gamma)\text{Cd}^{114}$ photoelectric coincidence spectrum observed in Arrangement B under the same conditions as the data shown in Fig. 10.

²⁴ B. J. Dropesky and A. W. Schardt (to be published).

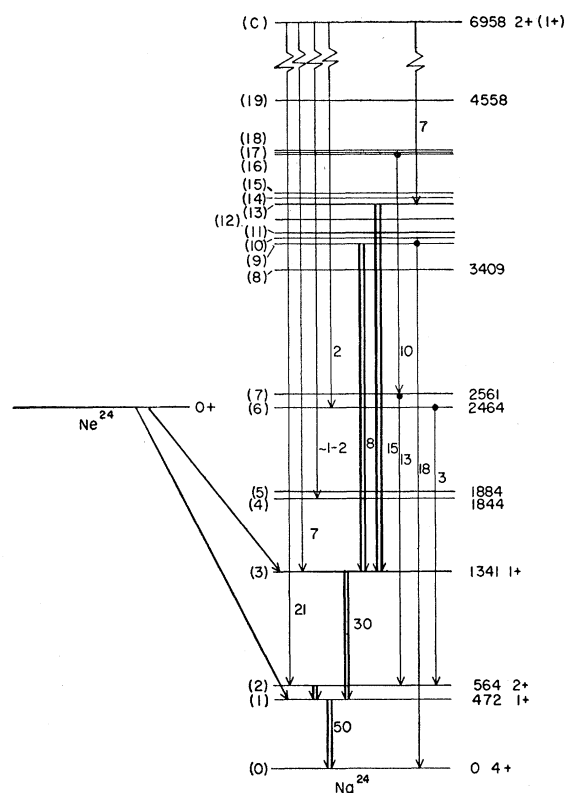


FIG. 12. Decay scheme of Na^{24} . The level numbers at the left and the energy values (in keV) on the right are from $\text{Na}^{23}(d,p)\text{Na}^{24}$.²¹ The Ne^{24} decay scheme is from Droupesky and Schardt, reference 24. The four transitions from the capturing state (C) to various levels are from Kinsey *et al.*, reference 23 and Groshev *et al.*, reference 4. The five double-line transitions are considered definite assignments of transitions observed in the present work and the five single-line transitions on the right are possible assignments of additional low-energy lines. The figures next to the transitions are the line strength in gamma rays per 100 neutrons captured. The spin assignments for states (1), (2), and (3) are from reference 24.

for the first three levels are in agreement with the angular distribution studies of $\text{Na}^{23}(d,p)\text{Na}^{24}$ for states (1+2) and (3).²⁵

Na^{24} is an odd-odd nucleus and detailed theoretical predictions of the character and energies of the excited states are not available owing to the many possible interactions expected between the odd nucleons. According to the shell model, the ground-state proton configuration of Na^{23} is $(d_{5/2})^3$ and the measured spin is $\frac{3}{2}$.²⁶ Na^{24} is formed by the absorption of an s neutron to form an excited state at 6958 keV of spin 1+ or 2+. The first known neutron resonance of sodium forms a state of spin 2²⁷ and it is certain that some large fraction of the state (C) must then be composed of a 2+ state. The existence of a spin 1+ excitation from an appreci-

able fraction of slow neutron absorption cannot be eliminated, however. The decay of the excited state (C) must be expected to show extreme variations from any predictions made from a single nucleon transition even if it is wholly 2+ and one cannot use the spin change as a reliable guide in estimating the strength of a transition from this state. It is probably because of this complex nature that the predicted $M1$ transition (C)–(1) is not observed to occur in the work of Kinsey *et al.*²² and of Groshev *et al.*⁴ even though the $M1$ transitions (C)–(2) and (C)–(3) are seen from their data. Because of these considerations and also because of the incomplete decay scheme based on the observed data, no definite spin assignments can be made for Na^{24} levels other than for the first three levels which are determined from the Ne^{24} decay.

5.2 Cadmium

The radioactive decay of In^{114m} excites Cd^{114} by means of a K -capture branch and two cascade gamma rays from Cd^{114} are emitted. The energy of these gamma rays has been reported as 556 ± 1 and 722 ± 1 keV¹¹ and recent angular correlation measurements¹⁴ assign to the spins 2 and 4 and even parity to the 556- and 1278-keV excited states. The strong line from $\text{Cd}^{113}(n,\gamma)\text{Cd}^{114}$ measured in this work to be 559 ± 2 keV corresponds to the expected $E2$ transition observed in the indium decay. The order of the two gamma rays is not known from the indium decay, but the high intensity of the lower energy line from the capture gamma-ray spectrum, the similarity of the level to other even A cadmium isotopes, and the Coulomb excitation observation of the state indicate with certainty that the first excited state of Cd^{114} is 559 keV as illustrated in Fig. 13.

The internal conversion line of 1305 ± 8 keV listed in Table I must correspond to a $0^+ - 0^+$ transition from a 0^+ state at 1305 ± 8 keV which is converted in competition with external gamma-ray emission to low-lying levels other than the 0^+ ground state. The 752-keV line fits well with the expected $E2$ transition from the 0^+ excited state to the first excited state at 559 keV. The 654-keV line observed in the external conversion spectrum is known from the internal conversion data to be $E2$ or perhaps $M1$ or $(M1+E2)$ and its intensity is such that it must be in cascade with the strong 559-keV transition. This would then suggest a state at 1213 keV. Another line is observed at 1210 keV and this is interpreted as the crossover transition from the same level to the ground state. Assuming such a crossover and stop-over decay, the weighted average for this state becomes 1212 ± 3 keV. It has previously been reported that a gamma ray of 95.7 ± 0.5 keV of either $E1$, $M1$, or $E2$ character is present in the $\text{Cd}^{113}(n,\gamma)\text{Cd}^{114}$ spectrum.¹³ This 95.7-keV transition fits well if it represents a transition between the 0^+ state at 1305 ± 8 and the 1212 ± 3 keV states. Assuming this mode of decay, the energy of the 0^+ state is 1308 ± 3

²⁵ P. Shapiro, Phys. Rev. **93**, 290 (1954); Bretscher, Alderman, Elwyn, and Shull, Phys. Rev. **96**, 103 (1954).

²⁶ J. E. Mack, Revs. Modern Phys. **22**, 64 (1950).

²⁷ Hibdon, Muehlhause, Selove, and Woolf, Phys. Rev. **77**, 730 (1950).

keV. The 1212-keV state is most likely $2+$ in accordance with the general character of the low-lying states of even-even nuclei. The internal conversion data for the 95.7- and 654-keV transitions cannot, however, exclude a $1+$ assignment for the 1212-keV state and the observed intensity of the 95.7-keV transition relative to the 752-keV $E2$ transition indicates that it is probably $M1$ which suggests a $1+$ assignment.

The transition probability of $0^+ \rightarrow 0^+$ transitions has been calculated by Church and Weneser by assuming that the strength parameter ρ is unity, and has been compared to single proton transition rates.²⁸ The Cd^{114} decay scheme allows an estimate of the 1308-keV $0^+ \rightarrow 0^+$ transition probability relative to assumed 95.7- and 752-keV transition rates. Assuming that both of these transitions are $E2$ and that the transition rates are those ascribed to single proton transitions,²⁹ then the total transition probability of the monopole conversion is $\sim 2 \times 10^9 \text{ sec}^{-1}$. The value given by Church and Weneser for monopole K conversion is $\sim 5 \times 10^9 \text{ sec}^{-1}$.

Kinsey and Bartholomew³⁰ have observed three incompletely resolved high-energy lines from cadmium with intensities of 0.12, 0.16, and 0.21% gammas per neutron captured and these lines correspond to excited states of 1205 ± 14 , 1320 ± 11 , and 1381 ± 11 keV if it is assumed that these high-energy lines are emitted from the $1+$ capturing state of Cd^{114} . The state at 1212 ± 3 keV discussed above agrees well with the first of these values and the 0^+ state at 1308 ± 3 keV agrees with the second. If the 808 ± 3 and 1370 ± 5 keV lines listed in Table III are assumed to come from a state at 1368 ± 4 keV, then such a state would be consistent with the third value predicted by Kinsey and Bartholomew. The 1368-keV state then has a spin of 1 or 2 since it is excited by the $1+$ capturing state and decays to both the $2+$ excited state and to the 0^+ ground state. The internal conversion data of Table I indicate that the 808 transition is either $M1$ or $E2$ and this is consistent with either a $1+$ or $2+$ assignment for the 1368-keV level. The assignment $2+$ to this level is preferred for an even-even nucleus and three of the states 1212 ($2+$), 1308 (0^+), 1368 ($2+$), and 1286 ($4+$) could be interpreted as a 0^+ , $2+$, $4+$ "triplet" as predicted in the "free vibration" model of Scharff-Goldhaber and Weneser.³¹ The high-energy lines observed by Adyasevich *et al.*⁵ indicate the excitation of states at 1180 ± 60 and 1330 ± 60 keV but these data do not agree in such detail as those of Kinsey and Bartholomew with the preferred scheme illustrated in

²⁸ E. L. Church and J. Weneser, Phys. Rev. **100**, 943 (1955); **103**, 1035 (1956).

²⁹ S. A. Moszkowski in *Beta- and Gamma-Ray Spectroscopy*, edited by K. Siegbahn (North Holland Publishing Company, Amsterdam, 1955), Chap. 13.

³⁰ B. B. Kinsey and G. A. Bartholomew, Can. J. Phys. **31**, 1051 (1953).

³¹ G. Scharff-Goldhaber and J. Weneser, Phys. Rev. **98**, 212 (1955).

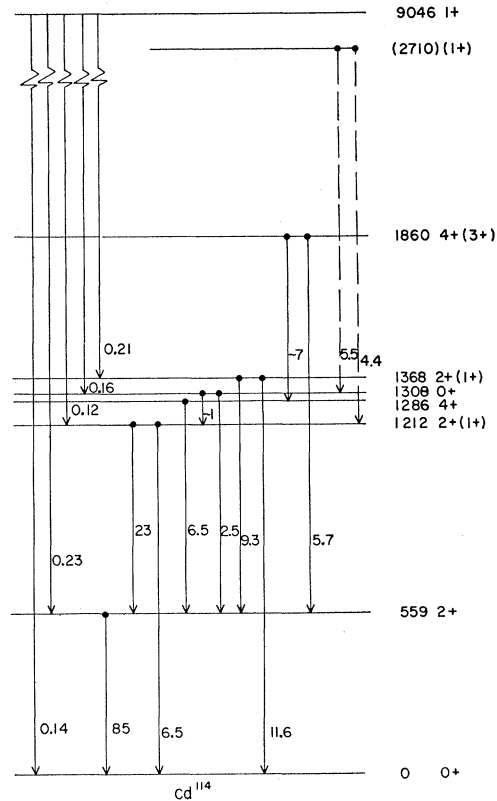


FIG. 13. Decay scheme of Cd^{114} . The five transitions from the capturing state indicated on the left are from Kinsey and Bartholomew, reference 30. See text for the assignment of the twelve low-energy transitions and the indicated spin assignments. The numbers next to the transitions are the observed gamma-ray intensities in gamma rays per 100 neutrons captured.

Fig. 13. Adyasevich *et al.* have observed 37 lines from cadmium, and 34 of these have been assigned to 51 transitions in their proposed decay scheme. The dual and triple assignment of 13 lines in this decay scheme clearly indicates the arbitrary nature of their proposed scheme.

The gamma rays of 576 and 1298 keV have an energy difference of 722 ± 7 keV and they are assumed on this basis to come from a state of spin 3 or 4 with even parity at 1860 ± 5 keV. Johns *et al.* have previously reported that a state in Cd^{114} at 1856 ± 4 keV is excited in the K -capture branch of In^{114} .^{11,32} It has recently been shown, however, that the 1300-keV gamma ray from In^{114} belongs to Sn^{114} and not Cd^{114} ,^{33,34} and that no excited state in Cd^{114} of energy greater than 1650 keV can be excited by In^{114m} .³³ Adyasevich⁵ reports a weak high-energy gamma ray that most likely leads to a state at 1920 ± 60 keV. The spin assignment of 3 or 4 and even parity for the 1860-keV level proposed here predicts an $E2$ or $M3$ transition from the $1+$ capturing

³² Johns, McMullen, Donnelly, and Nablo, Can. J. Phys. **32**, 35 (1954).

³³ L. Grodzins and H. T. Motz, Phys. Rev. **102**, 761 (1956).

³⁴ Johns, Williams, and Brodie, Can. J. Phys. **34**, 137 (1955).

state and so is not expected to be excited directly with an intensity comparable with the $M1$ transitions exciting the $0+$, $1+$, or $2+$ levels. It is therefore doubtful that the line observed by Adyasevich excites the state of 1860 ($4+$, $3+$). The intensity of the high-energy $M1$ transitions is at most 0.6% gammas per neutron captured whereas the weakest low-energy line that can be detected with the present equipment is $>1\%$. Thus excitation in addition to a direct transition from the capturing state is required and it is possible that the low-energy data might miss the de-excitation of a weakly populated state and this is indeed suggested by the unaccounted for x-rays observed.

The gamma rays of 1403 and 1498 keV have an energy difference of 95 ± 7 keV and fit energetically into the decay scheme assumed to come from a state at 2710 ± 6 keV with spin 1 and even parity. Such a state should be excited directly by means of an $M1$ transition from the capturing state but no such high-energy transition is observed by either Kinsey and Bartholomew³⁰ or by Adyasevich *et al.*⁵ It is, therefore,

uncertain that these lines actually originate from a $1+$ state at 2710 keV.

It is not possible to assign the higher energy lines observed in this work with sufficient reliability merely on an energy balance argument. Greater precision and resolution or coincidence experiments are necessary to complete the decay scheme above 2-MeV excitation. Measurements on $\text{Cd}^{113}(d,p)\text{Cd}^{114}$ would be of great value in verifying and extending the decay scheme. Muehlhause¹ has observed that an average of 4.1 cascade gamma rays are emitted in the $\text{Cd}^{113}(n,\gamma)\text{Cd}^{114}$ reaction and it must be expected that the coincidence spectrum will be very complex.

ACKNOWLEDGMENTS

The author gratefully acknowledges the many helpful discussions and encouragement given him by Dr. G. Scharff-Goldhaber, Dr. M. Goldhaber, and Dr. D. E. Alburger. He is also indebted to several members of the Electronics Division for the design and construction of equipment and to the consistent assistance of the Reactor Operations Group.

Dependence of the Pure Quadrupole Resonance Frequency on Pressure and Temperature*

T. KUSHIDA,† G. B. BENEDEK, AND N. BLOEMBERGEN

Division of Engineering and Applied Physics, Harvard University, Cambridge, Massachusetts

(Received August 29, 1956)

Measurements of the pure quadrupole resonance frequency (ν) of the Cu^{63} nucleus in cuprous oxide, and the Cl^{35} nucleus in potassium chlorate and paradichlorobenzene have been made as a function of pressure in the range 1 to 10 000 kg/cm² for temperatures between -77°C and 100°C . A theory is presented in which the static value of the electric field gradient tensor (ϕ_{ii}^0) and the amplitudes ξ_i^0 of the normal modes of the lattice vibrations play a central role. The volume dependence of these quantities can be deduced from ν -versus-volume isotherms which are constructed from the experimental data by using the equation of state. Information on the latter is augmented by theory. It is found that the temperature variation of the resonance frequency at atmospheric pressure can be understood by considering not only the explicit temperature dependence of the vibration amplitudes, but also by including the appreciable effects of the volume expansion on q_0 and ξ_i^0 . Furthermore, the pressure dependence is found to be explicable in terms of the volume dependence of q_0 and ξ_i^0 . In Cu_2O , it is found that q_0 depends on volume roughly as V^{-1} , thereby indicating an ionic character for this crystal. On the other hand, in paradichlorobenzene, $q_0 \propto V^n$, with $0 < n < 0.04$, thus exhibiting the effect of an increase in the intermolecular hybridization of the C-Cl covalent bond.

I. INTRODUCTION

SINCE its discovery,¹ the pure quadrupole splitting of the nuclear spin energy levels in solids has been investigated as a function of temperature. Bayer² proposed a theory, later generalized by Kushida³ and Wang,⁴ which explained the salient features of this

effect. It failed, however, to give detailed agreement with experiment.⁵ According to this theory, the average internal field gradient at the nucleus decreases with increasing temperature solely because of the increase in the amplitude of the thermal vibrations.

It seems fairly obvious that a strain deformation at constant temperature will also alter the electric field gradients in the solid lattice. Uniaxial compression in cubic crystals was first attempted by Watkins and

* This research was supported by the Office of Naval Research, the Signal Corps of the U. S. Army, and the U. S. Air Force.

† On leave of absence from the Department of Physics, Hiroshima University, Hiroshima, Japan.

¹ H. G. Dehmelt and H. Krüger, *Z. Physik* **129**, 401 (1951).

² H. Bayer, *Z. Physik* **130**, 227 (1951).

³ T. Kushida, *J. Sci. Hiroshima Univ.* **A19**, 327 (1955).

⁴ T. Wang, *Phys. Rev.* **99**, 566 (1955).

⁵ Dautreppe, Dreyfus, and Soutif, *Compt. rend.* **238**, 2309 (1954).